

# Experimental study on monotonic straight shear of grouted pile-ring beam node with U-bar connection

Yuan Shiwei<sup>1</sup>, Wang Weizhe<sup>1</sup>

<sup>1</sup>Structural Engineering, University of Shanghai for Science and Technology, Shanghai, 200093, China

---

## Abstract

In order to solve the problem of the connection of the pile-ring-beam node in the pile-column integration, a U-bar connection of the pile-ring-beam node was designed. The mechanical properties of the node were investigated by designing 1:1 specimens and conducting static loading tests in the field to verify the displacement of the crossbeam and ring beam, the crack development process, and the reinforcement strain of the node under different levels of loading. The test results show that there is no significant slip at the interface of the U-bar connected pile-ring beam node, and the interface connection is reliable. The damage pattern of the specimen showed that the specimen could not hold the load when it was loaded to the destructive load, the tensile longitudinal tendons at the outer side of the ring girder yielded, the plastic hinge was formed at the end of the cross girder, and the ductile damage occurred at the interface between the ring girder and the cross girder of the specimen. The cracking load of the specimen is 30T and the destructive load is 130T, and the load calculation formula of the node is obtained, and the results of the study can provide a reference for the node connection of the pile-ring girder node, and promote the engineering application of the node connection of the beam-column node in the pile-column integration.

**Keywords:** Pile-column integration, U-bar connection, ring beam node, straight shear, bearing capacity.

---

Date of Submission: 09-12-2023

Date of acceptance: 23-12-2023

---

## I. INTRODUCTION

Concrete-filled pile-ring beam node has the advantages of good mechanical properties, easy construction and low cost, while the connection performance between pile column and beam is the key to influence the safety of the structure, for which it has received extensive attention. Lv Wenlong et al [1] used straight bars for the connection between old columns and new beam nodes, and the study showed that the interface bars in this connection effectively transferred the shear force at the beam end, and there was no shear damage between the old and new concrete at the beam end. Gerson et al. [2] used ANSYS software to establish a finite element model of reinforced concrete beam-circular steel pipe concrete column ring beam node, by simplifying the compressive stress distribution of concrete in the compression zone of the ring beam, the node bending capacity design formula was derived, and the results showed that the magnitude of the torque of the ring beam under the action of the bending moment is affected by the ratio of the width of the frame beam and the radius of the steel pipe, and the bigger the ratio is, the smaller the torque is. Zhou Ying et al [3] conducted an experimental study on seven steel-tube concrete stacked column edge node ring beams, and monotonic static loading test was applied to two of the specimens, which showed that the larger the reinforcement ratio is, the more prone the node is to frame beam damage. Yu Feng et al [4] analysed the PVC-CFRP pipe concrete column-reinforced concrete ring beam nodes under low perimeter repeated loads by using fibre model method based on experimental study and the results showed that the increase in the strength of concrete in the core area decreases the ductility of the nodes. Pan Sheng et al [5] analysed the prestressed concrete ring girder node using finite element software and concluded that the shear bearing capacity of the node can be increased by increasing the prestressing force. Ping Wu et al [6] carried out an experimental study on columns in RC ring girder nodes under eccentric loading and showed that the initial stiffness of the node increased with the decrease in the height of the ring girder. Yu Feng et al [7] by varying the reinforcement ratio of the ring girder and the width of the ring girder, effectively increased the node bearing capacity of the node. Yu Feng et al increased the node bearing capacity and slowed down the degradation of strength and stiffness by changing the ring beam reinforcement ratio and ring beam width. Chen Yihu et al. [8] concluded from the test that the beam end node assembled with new U-shaped steel ring connection has slower crack development and better ductility than ordinary cast-in-place beams. Jiao Anliang et al [9-10] conducted seismic tests on assembled shear walls with U-bar lap connections and studied the effects of insert diameter, U-bar lap location and lap height on the force performance of the U-bar lap connection, which showed that the U-bar lap connection can meet the anchorage requirements and can be popularised and applied in the project.

As a new type of node connection, U-bar lap connection has been applied to actual projects. However, at present, no complete theory has been established for the calculation of bearing capacity and so on for the ring-beam node with one pile-column. Zhang Xizhi et al [11] conducted axial tensile test on wall specimens with U-bar lap connection, but only for the anchorage performance of U-bar in tension, without considering the actual engineering U-bar in shear.

In view of the shortcomings of the existing research, this paper carries out static loading test on two foot-size 1:1 specimens with U-bar connection in the node of filled piles - ring beam, to analyse the influence of concrete strength and U-bar diameter and other parameters on the performance of the U-bar overlap connection, and through the analysis of the experimental data, to establish the calculation formula of the bearing capacity of the U-bar overlap connection under the action of static loading, with a view to guiding the application of the project.

**1.1 Specimen design and fabrication**

The two specimens of this test have the same cross-section size and reinforcement, as shown in the figure, the cross-section size of the grouted pile  $\Phi=850\text{mm}$ , reinforcement: longitudinal bar 28 C 32, hoop bar A6@200; ring beam cross-section size of  $b=500\text{mm}, h=1000\text{mm}$  reinforcement: longitudinal bar 6C25; cross beam cross-section size of  $b=500\text{mm}, h=900\text{mm}$ , reinforcement: upper and lower longitudinal bar 7C28, hoop bar A8@400, A8@200, and waist bar 6A16. A8@400, A8@200, waist bar 6A16, and then on the basis of interface chiseling treatment, also in the pile body pre-buried A16 U-type shear reinforcement, set into the upper and lower two rows of cross-arrangement. The position of the specimen reinforcement and the basic parameters of the nodes are shown in Table 1 and Fig. 1.

**Table 1 :Basic parameters of each specimen**

test piece	b /mm	h /mm	f <sub>cu</sub> /(N·mm <sup>-2</sup> )	Upper longitudinal bar		Lower longitudinal bar		hooped bar		lumbar muscles		tension bar	
				quantities	f <sub>y</sub> /(N·mm <sup>-2</sup> )	quantities	f <sub>y</sub> /(N·mm <sup>-2</sup> )	quantities	f <sub>y</sub> /(N·mm <sup>-2</sup> )	quantities	f <sub>y</sub> /(N·mm <sup>-2</sup> )	quantities	f <sub>y</sub> /(N·mm <sup>-2</sup> )
ring girder	500	1000	17.7	10C22	385.8	10C22	385.8	$\Phi 14@280$	377.9	$\Phi 14@150$	377.9	$\Phi 14@560$	377.9
crossbeam	500	900	17.7	5C28	386.5	5C28	386.5	$\Phi 12@160$	225.6	6 $\Phi 12$	225.6	$\Phi 12@320$	225.6

- Note: ① b and h in the table are the width and height of the ring beam section respectively.  
 ② f<sub>cu</sub> is the measured cubic compressive strength of concrete, the average value of cubic strength measured by two 150×150×150mm cubic specimens cured under the same conditions as the specimen on the day of the experiment.  
 ③ The upper and lower longitudinal bars and ring beam waist bars and tension bars are HRB400 grade steel bars, and the cross beam hoop bars, waist bars, tension bars and ring beam hoop bars are HPB235 grade steel bars.

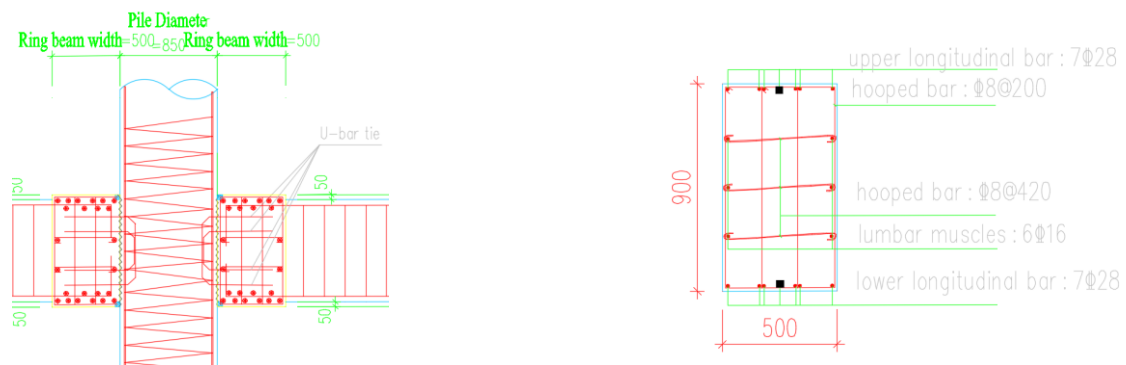


**Figure1: Cross-sectional dimensions and reinforcement of each specimen**

**1.2 Test loading programme**

In order to simulate the straight shear stresses between the ring beams and the filled piles under different conditions in the actual project, the ages of the concrete used in the 2 specimens in this paper are slightly different. In order to facilitate the loading, a 1:1 counterforce beam was fabricated as part of the loading device during the field test, and the loading scheme of the 2 specimens is shown in Fig. 1, and the actual loading scheme is shown in Fig. 2. In order to observe the location and development of the cracks in the ring beam and cross beam during the loading process, as well as the changes and distribution of the ring reinforcement hoop and longitudinal bars of the ring beam nodes, longitudinal bars of the cross beam and the U-bars strains with the load, and at the same time, in order to visually observe the magnitude of the relative slips of the pile columns

and the ring beams during the loading process, a monotonous straight-shear loading scheme of static grading until damage was adopted in the present test.

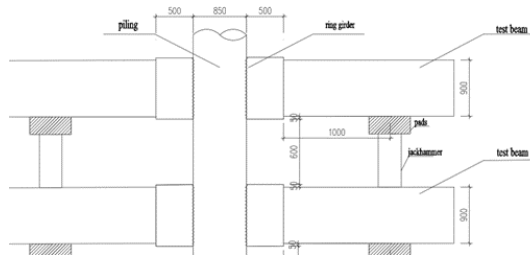


Figure 2 : Test loading programme

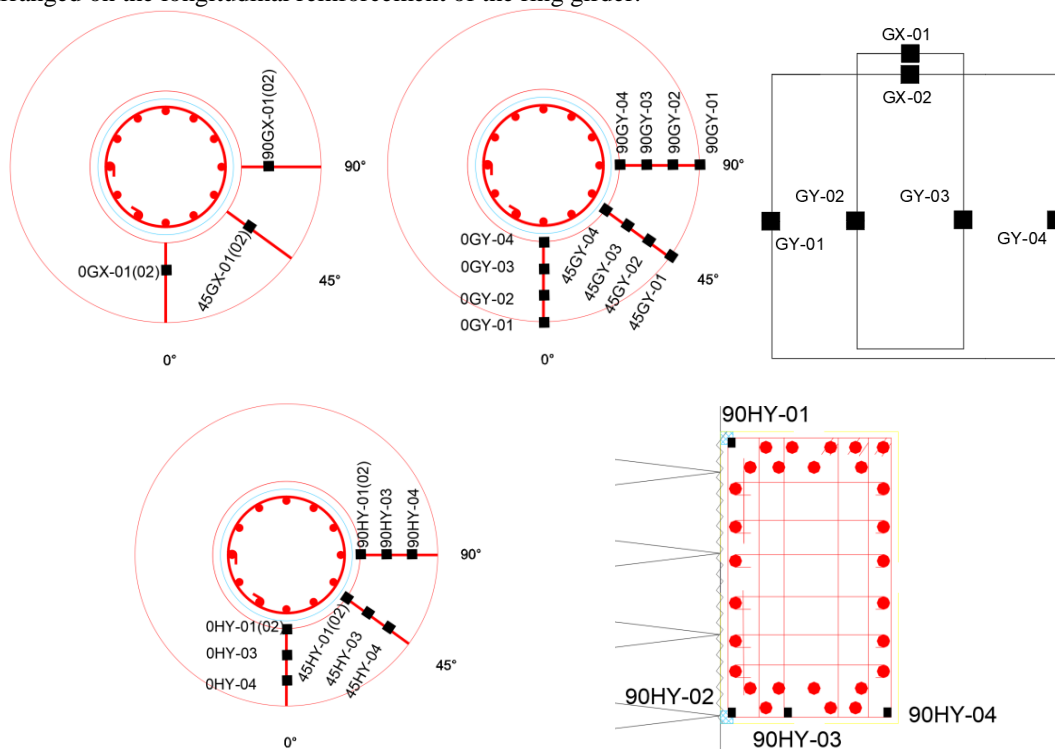


Figure 3 : Test loading programme

### 1.3 Main measurements

#### 1.3.1 Strain magnitude and distribution of longitudinal reinforcement and hoop reinforcement at the top and bottom of the ring girder

In order to analyse the stress performance of the ring girder, in this paper, 18 strain gauges were uniformly arranged on the hoop reinforcement of the ring girder, while 12 strain gauges were uniformly arranged on the longitudinal reinforcement of the ring girder.

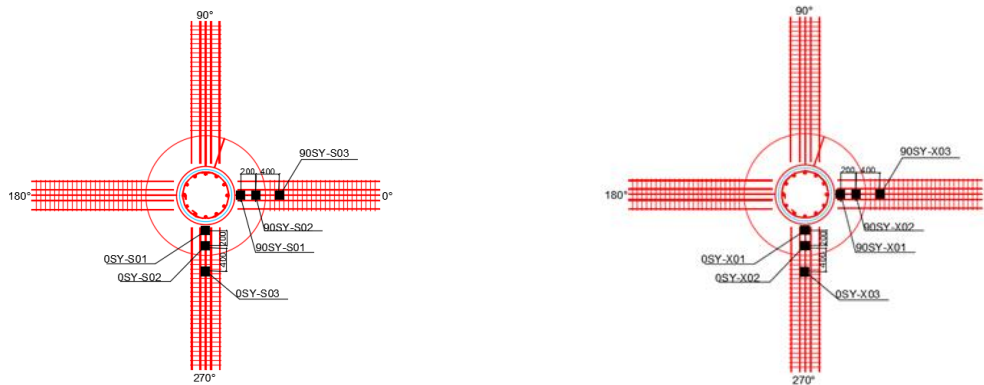


(a) Arrangement of hoop strain measurement points

(b) Arrangement of strain measurement points for longitudinal tendons of ring beams

#### 1.3.2 Strain magnitude and distribution in longitudinal bars of cross beams

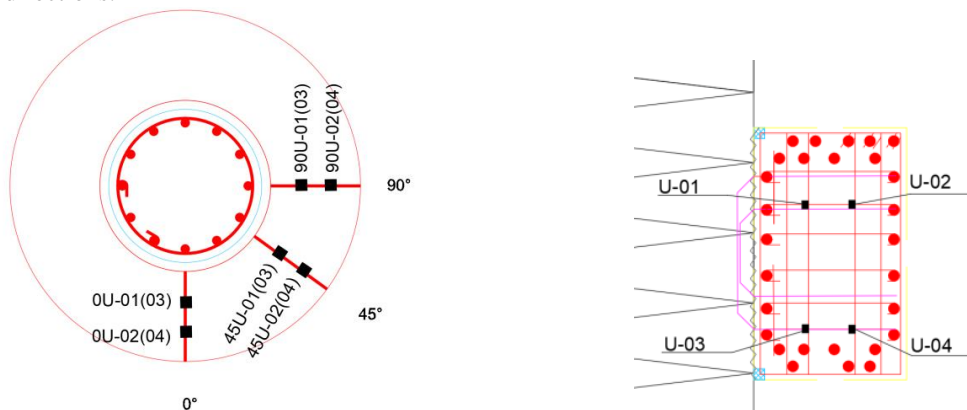
In order to analyse the stress performance of the crossbeam, 12 strain gauges were uniformly arranged on the longitudinal bars of the crossbeam, among which the measurement points 0SY-S and 90SY-S were used for observing the strain of the upper skinned longitudinal bars of the crossbeam in different directions, and the measurement points 0SY-X and 90SY-X were used for observing the strain of the lower skinned longitudinal bars of the crossbeam in different directions as shown in the figure below.



(c) Layout of strain measurement points on the upper (lower) surface of longitudinal bars of cross beams

### 1.3.3 Strain magnitude and distribution in U-bars

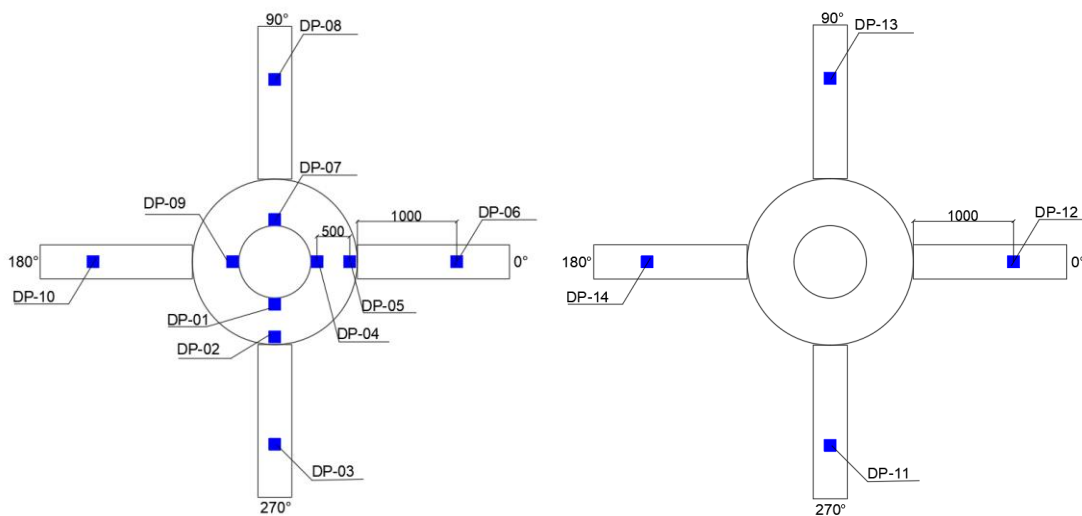
In addition, 12 U-bar strain measurement points were arranged to observe the U-bar strains in 3 different directions.



(d) Arrangement of strain measurement points for U-bars

### 1.3.4 Deformation observation

During the test, a total of 15 deformation observation points were arranged to measure the deformation at the combined surface of the ring beam and pile column, the outer edge of the ring beam, the loading point of the cross beam and the base of the jack, as shown in the figure below.



(e) Layout of test piece deformation measurement points

Fig. 4 :Arrangement of test points and section diagram of each specimen

## 2. Test results and analyses

### 2.1 Force analysis of the nodes before the specimen enters the damage

From the test loading load continued to increase, there was a tendency for the ring girder and the grouted piles to slip relative to each other. As the load continues to increase, cracks appear at the lower edge of the junction between the side of the ring girder and the cross girder, and diagonal cracks appear at the loading point of the side of the cross girder, and the concrete on the lower surface of the ring girder is crushed, and at this time the straight shear capacity of the node does not decrease, indicating that the local compression damage of the concrete on the lower surface of the lower surface of the concrete in this paper is not a cause of the specimens to reach the maximum bearing capacity of straight shear. As the ring beam cross-section of the upper and lower parts of the preparation of a certain number of ring longitudinal reinforcement, ring longitudinal reinforcement and hoop reinforcement together to form a skeleton that can restrain the radial deformation of the ring beam concrete, and the ring beam itself has a sufficient cross-section width, so that, although the ring beam has a tendency to slip upward and expand along the radial direction, the formation of a number of cracks in the outer surface of the ring beam, as shown in Fig. 10 and Fig. 11, but the cracks on the surface of the ring beam are However, the cracks on the surface of the ring girder are very small, which indicates that there is no possibility of radial deformation splitting damage of the ring girder in the two specimens of this test. With the gradual increase of the load, the tension of the outermost ring reinforcement that restrains the radial expansion of the ring beam concrete increases gradually and enters yielding one after another, and the test specimen is about to enter the stage of being unable to hold the load, and at this time, the relative slip between the ring beam and the pile column is shown in Fig. 5.

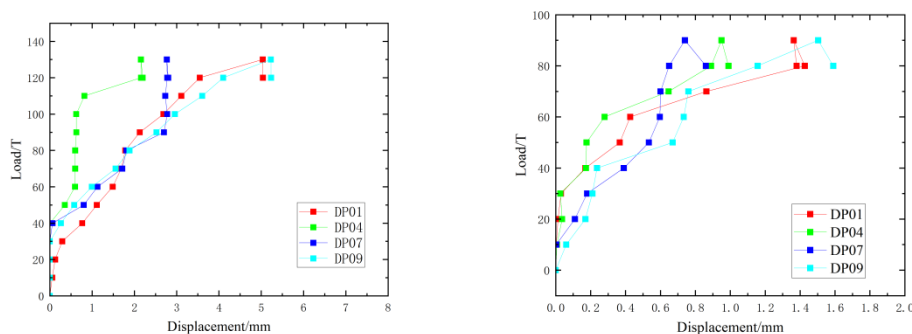


Fig. 5 :Load slip curve of each specimen

### 2.2 Force analysis of nodes when the specimen undergoes damage

According to the test results in this paper, the relative slip between the ring beam and the pile column will gradually increase and form a vertical slip surface after the concrete under the u-bars is locally crushed and forms a shaped surface there in the 2 specimens. However, the slip surface is not all generated between the ring beam and the pile wall, but as shown in Fig. 9, the slip surface is divided into two parts: the first part, above the first layer of u-bars in the upper part, the slip surface is generated between the ring beam and the pile wall; the other part is below the u-bars, and a vertical shear surface with a larger diameter is formed on the surface of the ring beam hoop reinforcement close to the pile part, and finally along this first ring shear surface, a straight shear damage occurs. Straight shear damage. This indicates that the pile is attached to the first layer of U-bars and the concrete layer between the ring beam hoop and the pile slides. The morphology of the upper and lower surfaces of the ring beam nodes after the damage of each specimen is shown in Fig. 6. Fig. 6 (a) shows the damage pattern of specimen a after reaching the ultimate load capacity, and (b) shows the damage pattern of specimen b after reaching the ultimate load capacity.

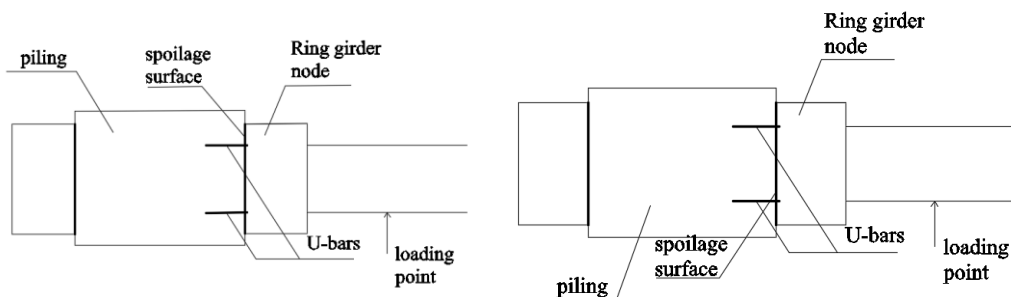


Fig. 6: Loading cross beams

When the test load of a single crossbeam reaches 400kN, specimen A cracks, microcracks appear on the side of the crossbeam, and diagonal cracks appear on the side of the ring beam at the lower edge of the junction with the crossbeam. When the test load of a single crossbeam reaches 50kN, the diagonal cracks on the side of the ring girder increase, diagonal cracks appear at the loading point on the side of the crossbeam, and transverse penetration cracks appear at the bottom of the crossbeam. At the bottom of the ring girder, ring and radial cracks in the direction of the ring girder diameter appeared. When loaded to 60kN, the diagonal cracks on both sides of the ring girder intersected, and the crack at the lower edge of the junction between the cross girder and the ring girder reached 0.701mm, the transverse cracks on the bottom surface of the cross girder increased, and the transverse cracks on the bottom surface of the cross girder and the ring girder junction reached 1.194mm. When loading a single cross girder from 80kN to 90kN, the load could not be held, and it was decided that the specimen was damaged, and the test was terminated. After observation, the concrete in the compression zone of the specimen was never crushed, and the interface between the ring beam and the grouted pile did not slip significantly. The cracks on the surface of the test specimen were distributed as follows: the maximum circumferential crack on the bottom surface of the ring girder was 1.387mm, the maximum radial crack on the bottom surface of the ring girder along the direction of the ring girder diameter was 0.545mm, the maximum diagonal crack on the side surface of the ring girder was 0.577mm, and the maximum transverse crack on the bottom surface of the cross girder was 2.063mm. when the test load of single cross girder reaches 30kN, the test specimen B cracks and the lower edge of junction between the cross girder and ring girder side reaches 2.063mm. Cracks appeared at the lower edge of the lateral junction between the cross beam and the ring beam. When loaded to 40kN, the cracks at the lower edge of the junction between the side of the crossbeam and the ring girder increased and developed into diagonal cracks towards the side of the ring girder, and transverse cracks appeared at the bottom of the crossbeam joint. When the test load of a single cross girder reaches 50kN, radial cracks along the diameter direction of the ring girder appeared on the bottom surface of the ring girder, and the cracks at the lower edge of the junction between the cross girder and the ring girder side and the transverse cracks at the bottom surface of the cross girder became more frequent. Subsequently, when loaded to 60kN, the diagonal cracks on the side of the crossbeam increased, the transverse cracks on the bottom surface of the crossbeam penetrated in many places, and the radial cracks along the diameter direction of the ring girder increased on the bottom surface of the ring girder. When loaded to 70kN, radial cracks on the bottom surface of the ring girder along the diameter direction of the ring girder penetrated, and diagonal cracks appeared at the loading point on the side of the cross girder. When the test load of a single cross girder reaches 80kN, the vertical crack at the combined part of the cross girder reaches 0.356mm, and the diagonal cracks on both sides of the ring girder intersect. The radial crack at the bottom of the ring girder reaches 0.134 mm. When the loading reaches 90 kN, the diagonal crack at the side of the ring girder reaches 0.269 mm, and the radial crack at the bottom of the ring girder increases. When a single crossbeam was loaded from 120kN to 130kN, the load could not be held, and the final crack distribution on the surface of the specimen was as follows: diagonal crack at the lower edge of the junction between the crossbeam and the side of the ring girder reached a maximum of 2.419mm, transverse crack at the bottom of the crossbeam reached a maximum of 2.340mm, and the radial crack at the bottom of the ring girder reached a maximum of 1.217mm. after observing the specimen, the concrete in the pressure zone was not crushed, and the interface of the ring girder and the piles increased to 0.269mm. There was no obvious slip at the interface between the ring beam and the grouted pile.

The test results show that the ultimate straight shear capacity of test specimen A is 90kN, and the concrete of test specimen B reaches 120kN due to the longer curing time, which is a significant improvement compared with test specimen A. Meanwhile, the load-displacement curves of each test specimen show that the displacement of test specimen A in reaching the ultimate straight shear capacity is obviously reduced compared with that of test specimen B. In addition, for the nodes in the actual structure, the most unfavourable load condition for straight shear damage between ring beam and pile is that the floor has a large vertical load, and then the cross beam with the ring beam banana is transmitted to the ring beam and pile. In addition, for the nodes in the actual structure, the most unfavourable loading condition for the occurrence of straight shear damage between the ring beam and the pile columns is the large vertical load on the floor, and at this time, the cross beams with the ring beam banana transmit negative moments to the ring beam. Setting the U-bars in the compression zone under the bending moment of the crossbeam is more favourable for resisting straight shear, and is more effective in reducing slip and improving the slip-resisting stiffness. Therefore, the setting scheme of U-bars in the two specimens of this test is more reasonable.

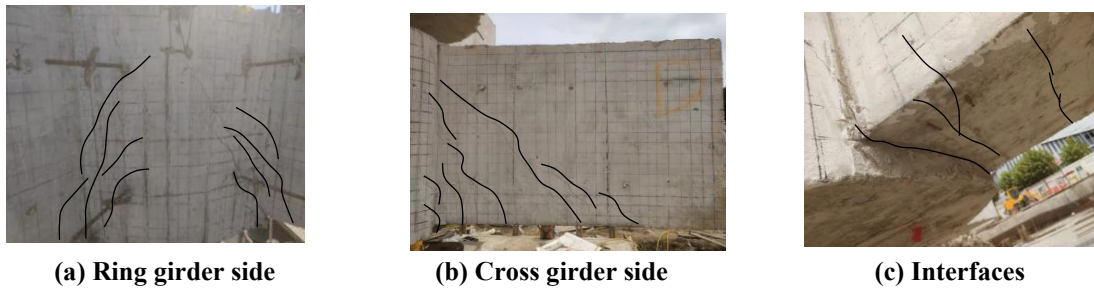


Fig. 10: Final damage pattern of specimen A

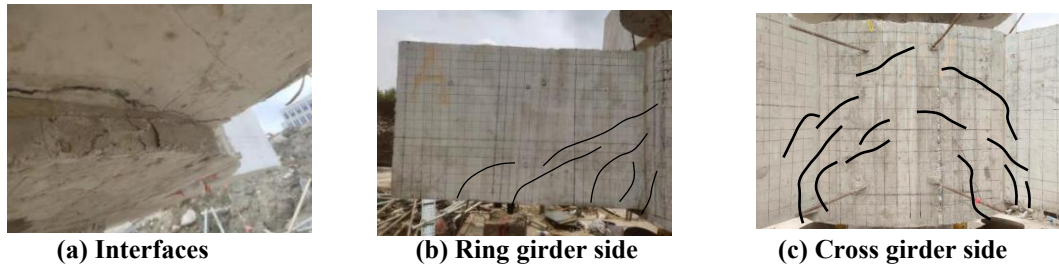


Fig. 11: Final damage pattern of specimen B

### 3. Load-strain curve analysis of steel reinforcement

During the test, the strains of hoop reinforcement, crossbeam longitudinal reinforcement, ring beam longitudinal reinforcement and U-shaped reinforcement in each direction of the specimen did not differ much, and the 0° direction was chosen to draw the load-strain curve of the reinforcement. The strain curves of the hoop reinforcement of the ring beam are shown in Fig. 12.

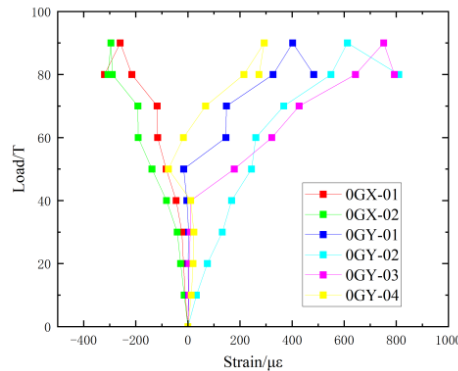


Fig. 12: Load-strain curve of hoop reinforcement of ring girder

Specimen in the beginning of loading, ring beam hoop did not force, has not produced strain, the load reached 30kN, the specimen cracking, cross beam and ring beam interface displacement, continue to hold the load to 40kN, the displacement continues to increase, due to the bonding effect of the concrete and reinforcement, the hoop began to force, the strain increases more slowly, when loaded to 80kN, the ring beam side diagonal cracks continue to develop to through, the hoop dramatically! Stressed, the strain increases rapidly, the curve tends to flatten until the end of loading, specimen destruction, the transverse section of the hoop and the vertical end of the strain has a certain difference, but in the final are not reached yield.

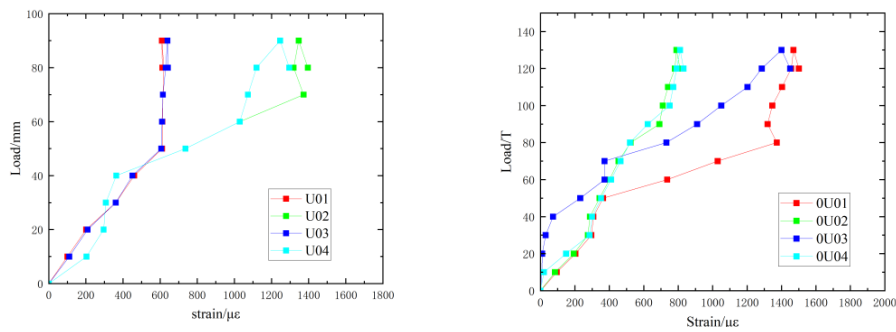


Fig. 13: Load-strain curve of U-bar

After the specimen cracking, the U-bar starts to be stressed, with the gradual increase of load, the growth rate of strain accelerates, and the growth rate of strain on the outside of the U-bar is smaller than that on the inside of the U-bar, and the strain on the outside of the U-bar is smaller than that on the inside of the U-bar, this is due to the fact that the inside of the U-bar is close to the interface of the crossbeam and the ring girder, and the angle of the inside of the U-bar with the shear stress is larger than that of the outside of the U-bar, so the change of the strain is Therefore, the strain change is greater. Before the end of load-holding, the U-bars all reach yielding.

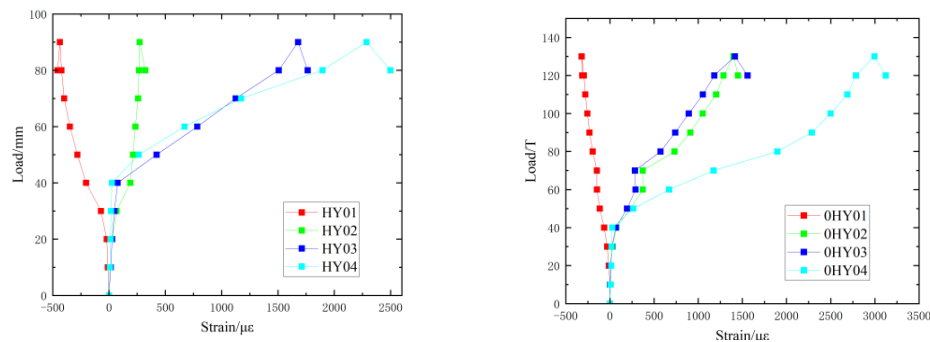


Figure 14: Load-strain curve of longitudinal reinforcement of ring girder

Ring beam longitudinal bars also in the load reached 40kN, gradually began to force, the inner upper longitudinal bar strain growth is more moderate, the outer longitudinal bar strain growth is more rapid, due to the different force area, the concrete ring beam outside and inside the stress size is different, and the outer longitudinal bar also need to bear the transverse tensile stresses, which leads to the outer longitudinal bar strain is greater than the inner side, in the load continues to increase to 130kN, and eventually When the load continues to increase to 130kN, the longitudinal reinforcement of the outer ring girder finally reaches yield.

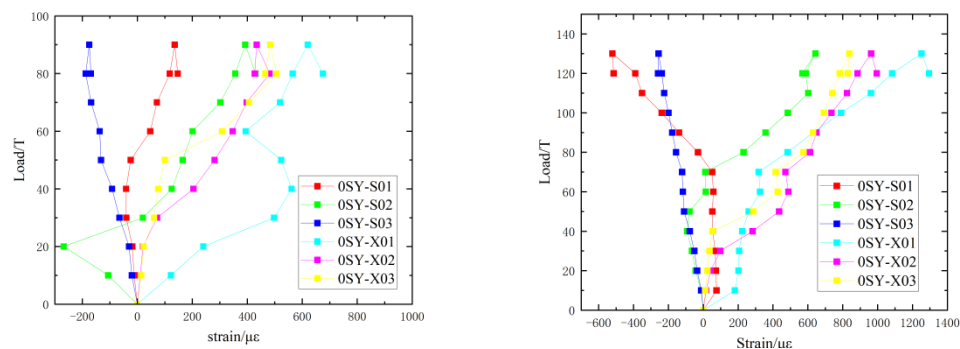


Fig. 15 Load-strain curve of longitudinal reinforcement of crossbeam

At the early stage of specimen loading, the strain of longitudinal bars of cross beams is very small, when the load of single cross beam reaches 80kN, the width of vertical cracks in the combined part increases rapidly, and part of the concrete withdraws from the work, and at this time, the stressed area of longitudinal bars increases, the curve becomes flat, and the strain increase is accelerated. The compressive strain of the longitudinal bars on the upper surface of the cross beam is negative, and the tensile strain of the longitudinal

bars on the lower surface is positive, and both of them do not reach yield when the destructive load is finally reached.

#### 4. Straight shear damage pattern and ultimate bearing capacity of pile-column-ring-beam node

Reading the literature, several straight shear damage patterns of pile columns and ring girders were analysed, i.e.: (1) the length of the U-bar overlap was sufficient, the U-bar was stretched and the inserted bars were sheared; (2) the length of the U-bar overlap was insufficient, the concrete in the overlap area of the specimen was sheared, the horizontal inserted bars were sheared or sheared, and the U-bar was not stretched. The literature gives the corresponding tensile capacity calculation formulae according to these two damage modes, and the final tensile ultimate capacity of the ring beam node connected by U-bars is shown as follows:

$$R_j = V_c + V_s \tag{1}$$

$$V_c = \alpha(A_c - n \frac{\pi}{4} d^2) f_{kN} \tag{2}$$

$$V_s = 0.6n \frac{\pi}{4} d^2 f_y \tag{3}$$

Where  $R_j$  - Nodal tensile load capacity

$V_c$  - is the shear capacity of concrete in the overlap area

$V_s$  - is the horizontal insertion bar shear bearing capacity

$\alpha$  - for the concrete shear strength and tensile strength conversion factor, can be taken as  $\alpha = 1$

$A_c$  - is the area of the lap area

$n$  - is the number of horizontal rebar

$d$  - is the diameter of the horizontal rebar

$f_{kN}$  - is the design value of concrete tensile strength

$f_y$  - is the design value of the yield strength of the horizontal insertion bar

The literature straight shear capacity formula using the measured strength of the material calculated by the straight shear capacity  $V_c$  and  $V_s$  of various damage forms and this paper 2 specimens of the measured ultimate load capacity  $R$  as shown in the table, the literature calculated load capacity and measured load capacity comparison is shown in Table 2.

**Table 2: Measured and Calculated Straight Shear Bearing Capacity of Specimens**

Test piece	ge/ay	$c$ <i>kN</i>	$V_s$ <i>N</i>	$V_j$ <i>/k</i> <i>N</i>	$R$ <i>/k</i>	Shear capacity at beam end $V_s$ / <i>kN</i>
U-bar connection A	2	63.41	7	1	2	900
U-bar connection B	8	61.06	8	1	2	1300

As can be seen from the table, the measured shear capacity of the two specimens are smaller than the calculated shear capacity, and some of the difference is very large. Although the damage pattern tested in this paper is basically the same as that of the second ring girder concrete straight shear damage occurred in the above literature, the difference between the calculated value and the measured value is still very large; according to the bearing capacity determined by the local compressive strength of the concrete on the supporting surface of the U-bar and according to the bending capacity of the U-bar is obviously lower than that of the ring girder concrete straight shear damage occurred in the determination of shear bearing capacity. This is due to the ring girder node born straight shear damage, steel and concrete can not completely play a role at the same time, in the load-holding period, only part of the reinforcement to play the role of shear and flexural, high stress straight shear process of shear stress - shear displacement has a non-linear elastic characteristics. And in the process of straight shear test, with the dynamic change of the shear surface, the effective shear area is gradually reduced, which will lead to the measured bearing capacity is less than the calculated straight shear bearing capacity. This indicates that the straight shear damage pattern of concrete column-ring-beam nodes connected by U-bars and the calculation of the load carrying capacity still need to be further improved on the basis of the literature suggestions.

## II. CONCLUSION

(1)The test on the straight shear capacity of the concrete pile-ring beam node with two U-bars showed that under the ring beam reinforcement condition in this test, when the specimen reached the maximum capacity, the displacement between the pile column and the ring beam was small, which ensured that the ring beam could effectively transmit the vertical shear force from the single cross beam. The load on the infilled pile-ring beam node connected by the U-bars meets the design requirements and the design of the pile-ring beam node with U-bars is not a problem. The load carried at the nodes of the pile-ring beam connected by U-bars meets the design requirements.

(2)As the ring beam cross-section of the upper and lower parts of the configuration of a certain number of ring beam and waist bars, these bars and ring beam hoop bars together to form a skeleton that can restrain the ring beam concrete deformation in the radial direction, as far as possible to load the late ring bar due to the expansion of the ring beam along the ring and part of the yield, but also to ensure that the ring beam will not occur in the radial cleavage damage. The damage of the specimens occurred at the end of the beam in the ring girder part. The performance of the ring beam longitudinal bars yielded in tension, the formation of plastic hinge at the end of the beam, the specimen occurred ductile damage. It can provide a reference basis for the design of the node of the pile-ring beam and promote the engineering application of the node of the beam-column connection in the pile-column integration.

(3)The straight shear damage model of the formula given in the literature is basically consistent with the damage of the test in this paper, but its calculated value is obviously higher than the measured value of the test in this paper. It shows that the calculation of bearing capacity needs to be further improved on the basis of the literature.

## REFERENCES

- [1]. Lv Wenlong, Shen Zhaoyong, Long Min. Experimental study on new ring-beam type node of reinforced concrete old column-new beam connection and its seismic performance[J]. *Industrial Building*, 2019, 49(04):187-190+186. DOI:10.13204/j.gygz201904030.
- [2]. Ge Sen, Nie Su Fei, Song Hong Yuan. Research on flexural design of reinforced concrete beam-circular steel pipe concrete column ring beam node[J]. *Building Structure*, 2014, 44(12):91-94+73. DOI:10.19701/j.jzjg.2014.12.018.
- [3]. Zhou Ying, Yu Haiyan, Qian Jiang et al. Experimental study of steel-tube concrete stacked column node ring beam[J]. *Journal of Building Structures*, 2015, 36(02):69-78. DOI:10.14006/j.jzjgxb.2015.02.009.
- [4]. Yu Feng, Maimaiti Nuraiti, Fang Yuan et al. Numerical simulation study on hysteresis characteristics of PVC-CFRP pipe-concrete column-RC ring-beam cruciform node[J/OL]. *Composites Science and Engineering: Cheng*:1-8[2023-12-19]. <http://kns.cnki.net/kcms/detail/10.1683.TU.20230427.1500.012.html>.
- [5]. PAN Sheng, FAN Lin, GUO Kuigang et al. Calculation and analysis of shear capacity of CCFST column-prestressed concrete ring beam node[J]. *Building Structure*, 2017, 47(S2):274-279. DOI:10.19701/j.jzjg.2017.s2.052.
- [6]. Wu P, Liu J, Yu F, et al. Flexural Stiffness Analysis of the PVC-CFRP-Confined Concrete Columns with RC Ring Beam Joint Under Eccentric Load[J]. *Iranian Journal of Science and Technology, Transactions of Civil Engineering*, 2021, 46(3).
- [7]. Feng Y, Shisi W, Yuan F, et al. Seismic behaviour of interior polyvinyl chloride-carbon fiber-reinforced polymer-confined concrete column-ring beam joints[J]. *Archives of Civil and Mechanical Engineering*, 2022, 23(1).
- [8]. Chen Yihu, Lu Dan, Zhang Min et al. Research on the performance of U-bar ring connection in assembled concrete beam-column nodes[J]. *Journal of Guangxi University(Natural Science Edition)*, 2019, 44(06):1552-1561. DOI:10.13624/j.cnki.issn.1001-7445.2019.1552.
- [9]. Jiao Anliang, Zhang Peng, Li Yonghui et al. Experimental study on seismic performance of prefabricated shear walls connected by ring bar buckling and anchor connection[J]. *Journal of Building Structures*, 2015, 36(05):103-109. DOI:10.14006/j.jzjgxb.2015.05.013.
- [10]. Jiao An-Liang, Zhang Peng, Gao Yufen et al. Mechanism study on anchorage performance of vertical connection reinforcement in assembled ring-bar buckled and anchored concrete shear wall[J]. *Industrial Building*, 2019, 49(01):69-76+129. DOI:10.13204/j.gygz201901013.
- [11]. Zhang Xizhi, Zhang Qunli, Gao Huachao et al. Study on the tensile bearing performance of precast concrete wall with U-bar lap connection[J]. *Journal of Building Structures*, 2021, 42(08):49-58. DOI:10.14006/j.jzjgxb.2019.0347.